

MMP-2 and MMP-9 synergize in promoting choroidal neovascularization

Vincent Lambert,* Ben Wielockx,[†] Carine Munaut,* Catherine Galopin,* Maud Jost,* Takeshi Itoh,[†] Zena Werb,[§] Andrew Baker,^{||} Claude Libert,[†] Hans-Willi Krell,[¶] Jean-Michel Foidart,* Agnès Noël,* and Jean-Marie Rakic[#]

*Laboratory of Tumor and Development Biology, University of Liège, Pathology Tower (B23), Sart-Tilman, B-4000 Liège; [†]Department of Molecular Biology, Flanders Interuniversity Institute for Biotechnology and University of Ghent, Ghent, Belgium; [‡]Shionogi Institute for Medical Science, Shionogi & Co., Osaka, Japan; [§]Department of Anatomy, University of California at San Francisco, San Francisco, California 94143; ^{||}Bristol Heart Institute, University of Bristol, Bristol Royal Infirmary, Bristol BS2 8HW, United Kingdom; [¶]Roche-Diagnostics GmbH, Pharma-Research Penzberg, 82372 Penzberg, Germany; and [#]Department of Ophthalmology, University Hospital, Sart-Tilman, B-4000 Liège, Belgium

Corresponding author: Jean-Michel Foidart, Laboratory of Tumor and Development Biology, University of Liège, Pathology Tower (B23), Sart-Tilman, B-4000 Liège, Belgium. E-mail: jmfoidart@ulg.ac.be

ABSTRACT

Matrix metalloproteinase 2 (MMP-2) and MMP-9 are increased in human choroidal neovascularization (CNV) occurring during the exudative most aggressive form of age-related macular degeneration (AMD), but their precise role and potential interactions remain unclear. To address the question of MMP-2 and MMP-9 functions, mice deficient in the expression of MMP-2 (MMP-2 KO), MMP-9 (MMP-9 KO), and both MMP-2 and MMP-9 (MMP-2,9 KO) with their corresponding wild-type mice (WT) underwent CNV induction by laser-induced rupture of the Bruch's membrane. Both the incidence and the severity of CNV were strongly attenuated in double deficient compared with single gene deficient mice or corresponding WT controls. The reduced neovascularization was accompanied by fibrinogen/fibrin accumulation. Furthermore, overexpression of the endogenous MMP inhibitors TIMP-1 or TIMP-2 (delivered by adenoviral vectors) in WT mice or daily injection of a synthetic and gelatinase selective MMP inhibitor (Ro 26-2853) significantly decreased the pathological reaction. These findings suggest that MMP-2 and MMP-9 may cooperate in the development of AMD and that their selective inhibition represents an alternative strategy for the treatment of choroidal neovascularization.

Key words: matrix metalloproteinase • CNV • age-related macular degeneration

The abrupt and often definitive loss of visual function resulting from choroidal neovascularization, which occurs in the exudative form of age-related macular degeneration (AMD), is a worldwide health problem with the aging population (1). It is estimated that by their 90s, one in four people will have lost vision from AMD (2).

Although the primary stimulus for the development of retinal neovascularization is hypoxia, the exact molecular signals involved in the appearance and growth of pathological choroidal neovascularization are not well defined (3). The net balance between positive and negative regulatory molecules controls angiogenesis (4). Vascular endothelial factor (VEGF) and pigment-epithelium derived factor (PEDF) are expressed in AMD and play an important role in choroidal neovascular membrane formation (5–7). Their contribution is further supported by the previous demonstration that either inhibition of the VEGF system or overexpression of PEDF efficiently inhibited choroidal neovascularization (8, 9). However, angiogenesis is also associated with an important extracellular remodeling involving different proteolytic systems, among which the matrix metalloproteinases (MMPs) play an essential role (10, 11).

The MMPs are a family of zinc- and calcium-dependent proteases that are capable of degrading the extracellular matrix (ECM) and basement membrane (10, 11). They are believed to play pivotal roles in embryonic development and growth (12, 13), as well as in tissue remodeling and repair (14, 15). Excessive or inappropriate expression of MMPs may therefore contribute to the pathogenesis of many tissue-destructive processes, including tumor progression (10, 11) and aneurysm formation (16). MMP effects are not restricted to ECM degradation (17). For example, peptide growth factors that are sequestered by ECM proteins become available once degraded by MMP-9 (18). MMPs can increase the bioavailability of VEGF (19) but also generate angiogenesis inhibitors such as angiostatin by cleavage of plasminogen (20).

A possible involvement of MMPs has been suggested in the progression of both retinal and choroidal neovascularization, and mutations in the TIMP-3 gene (tissue inhibitor of metalloproteinases-3) are the cause of a rare familial form of macular dystrophy associated with subretinal neovascularization (21–23). Using an experimental murine model of laser-induced choroidal neovascularization, we have recently demonstrated that MMP-9 secretion from inflammatory cells contributes to the development of pathological choroidal angiogenesis (24). The magnitude of angiogenesis inhibition produced by MMP-9 deficiency was, however, minor compared with that observed previously in the same model in mice deficient for plasminogen activator inhibitor type I (PAI-1; ref 25). This suggests that MMP-9 is not the only pathway for rendering angiogenic factors bioavailable, which clearly occurs in other experimental settings (19). Indeed, both MMP-9 and MMP-2 are expressed in human choroidal neovascular membranes removed during surgery for late stage AMD (26), while MMP-2 is the predominant MMP expressed during rat choroidal neovascularization formation (27). Furthermore, other investigators have pointed out that, depending on the specific context, these gelatinases could either work in concert or antagonistically (28, 29).

To address the question of MMP-2 and MMP-9 functions, we investigated the expression and activity of members of the MMP system in different stages of laser-induced murine choroidal neovascularization, comparing choroidal neovascularization formation in single (MMP-9 KO, MMP-2 KO) or double (MMP-2,9 KO) deficient mice compared with wild-type (WT) controls.

METHODS

Genetically modified mice

MMP-2^{-/-} mice (30) and MMP-9^{-/-} mice (13) were crossed with each other to obtain MMP-2^{+/-}MMP-9^{+/-} mice. These mice were intercrossed to obtain MMP-2^{-/-}MMP-9^{-/-} (double knockout, also designed as MMP-2,9 KO) and control wild-type (WT) MMP-2^{+/+}MMP-9^{+/+} mice. All mice were genotyped using PCR. Animal experiments were performed in compliance with the Association for Research in Vision and Ophthalmology (ARVO) statement for the Use of Animals in Ophthalmic and Vision Research. The animals were maintained with a 12:12-h light/dark cycle and had free access to food and water.

Experimental choroidal neovascularization

Choroidal neovascularization was induced in mice by four burns (usually at the 6, 9, 12, and 3 o'clock positions around the optic disc) using a green argon laser (532 nm; 50 μm diameter spot size; 0.05 sec duration; 400 mW) as previously described (24, 25). Mice with haemorrhage or not developing an evident bubble at the site of every laser impact (the sign of ruptured Bruch's membrane) were excluded from further analysis. Included animals (5 or more in each condition) were killed 14 days after laser (except for kinetic mRNA profiles). Before death, fluorescein angiograms (intraperitoneal injection of 0.3 ml of 1% fluorescein sodium, Ciba) were performed to confirm that laser burns were developing late phase increasing hyperfluorescent spots (corresponding to the leakage of fluorescein from newly formed permeable capillaries). The eyes were then enucleated and either fixed in buffered 3.5% formalin solution for routine histology or embedded in Tissue Tek (Miles Laboratories, Naperville, IL) and frozen in liquid nitrogen for cryostat sectioning. Choroidal neovascularization was quantified as previously described (24, 25). Briefly, frozen serial sections were cut throughout the entire extent of each burn, and the thickest region (minimum of 5/lesion) was selected for the quantification. With the use of a computer-assisted image analysis system (Olympus Micro Image version 3.0 for Windows 95/NT, Olympus Optical CO. Europe GmbH), neovascularization was estimated by the ratio (B/C) of the thickness from the bottom of the pigmented choroidal layer to the top of the neovascular membrane (B) to the thickness of the intact-pigmented choroid adjacent to the lesion (C). A mean B/C ratio value was attributed to each laser impact.

Gelatin zymography

Choroidal neovascularization was induced in mice by multiple burns ($n=30$) as described above. Animals were killed at different endpoints, and the eyes were enucleated. The posterior segments were cut out and immediately snap frozen in liquid nitrogen. Frozen tissues were then pulverized in liquid nitrogen, homogenized in buffer (0.1 M Tris-HCl, pH 8.1, 0.4% Triton X-100), and centrifuged for 20 min at 5000 g. The pellets were discarded. Aliquots of supernatants were mixed with SDS sample buffer and electrophoresed directly as described previously (31).

In situ zymography was performed by incubating cryosections (7 μm) with 40 μg/ml fluorescein-conjugated gelatin (Molecular Probes, Eugene, OR) in 50 mM Tris-HCl, pH 7.5, 10 mM CaCl₂, 150 mM NaCl, and 0.05% Brij-35 (Calbiochem) for 12 h at 37°C; sections were washed three

times with water and mounted with Vectashield. Gelatinase activity was visualized using fluorescent microscopy (32).

Immunohistochemistry

Cryostat sections (5 μm thick) were fixed in paraformaldehyde 1% in 0.07 M phosphate buffered saline (PBS), pH 7.0, for 5 min or in acetone for 10 min at room temperature and then incubated with the primary antibody. Antibodies raised against mouse PECAM (rat monoclonal, PharMingen, San Diego, CA; diluted 1/20), mouse MAC-3 (BD Pharming, San Diego, CA), and murine fibrinogen/fibrin (goat polyclonal, Nordic Immunological, Tilburg, The Netherlands; diluted 1/400) were incubated for 1 h at room temperature. The sections were washed in PBS (3x10 min) and appropriate secondary antibody conjugated to peroxidase (HRP) was added: rabbit anti-goat IgG (Dako, Glostrup, Denmark, diluted 1/100) and rabbit anti-rat IgG (Sigma-Aldrich; diluted 1/40) were applied for 30 min. For staining, a drop of AEC+ (Dako, 3-amino-9-ethylcarbazole) was added and sections were counterstained for 1 min in hematoxylin. Specificity of staining was assessed by substitution of nonimmune serum for primary antibody (not shown).

Adenovirus-mediated TIMP-1 and TIMP-2 gene transfer and synthetic MMP inhibitor treatment

Recombinant adenovirus bearing the gene coding for human TIMP-1 or TIMP-2 (AdTIMP-1, AdTIMP-2), or an empty control adenovirus (AdRR5) were generated as described previously (33–34). Twenty-four hours after laser spot production, mice were intravenously injected with 200 μl of adenovirus (7×10^8 PFU). On day 14, mice were killed and eyes were excised and processed as described above.

As an alternative way of MMP inhibition, WT mice were intraperitoneally injected with a broad spectrum MMP inhibitor (BB-94, British Biotech Pharmaceuticals Ltd., Oxford, UK) or a more selective inhibitor (Ro 28-2653, Roche-Diagnostics, Penzberg, Germany) interacting primarily with MMP-2, MMP-9, and MT1-MMP (35). The daily injections started either the same day as choroidal neovascularization induction (day 0) or at day 5.

RT-PCR analysis

To evaluate the kinetic of MMPs mRNA expression by semiquantitative RT-PCR, choroidal neovascularization was induced in mice by multiple argon laser burns and animals were killed at days 3, 5, 10, 14, 20, and 40. The posterior segments (RPE-choroid complex without neural retina) were cut out and immediately frozen in liquid nitrogen. rTth reverse transcriptase RNA PCR kit (Applied Biosystems, Foster City, CA) was used, and pairs of primers (Eurogentec, Liège, Belgium), oligonucleotides sequences, number of cycles, and expected PCR product size are shown in [Table 1](#). The frozen murine tissues were first pulverized using a Dismembrator (B. Braun Biotech international, GmbH Melsungen, Germany), and total RNA was extracted with the RNeasy extraction kit (Quiagen, Paris, France) according to the protocol of the manufacturer. 28S RNA was amplified with an aliquot of 10 ng of total RNA using the GeneAmp ThermoStable mRNA. Reverse transcription was performed at 70°C for 15 min followed by 2 min incubation at 95°C for denaturation of RNA-DNA heteroduplexes. Amplification started by

15 s at 94°C, 20 s at 60°C, and 10 s at 72°C. RT-PCR products were resolved on 2% agarose gels and analyzed using a Fluor-S MultiImager (Bio-Rad) after being stained with ethidium bromide (FMC BioProducts).

Statistical analysis

Data were analyzed with GraphPad Prism 3.0 (San Diego, CA). The chi-square and Mann-Whitney tests were used to determine significant ($P<0.01$) differences between WT and deficient mice.

RESULTS

Induction of experimental choroidal neovascularization in WT, MMP-2KO, MMP-9KO, and MMP-2,9KO mice

Fluorescein angiography performed before death ([Fig. 1F](#)) showed a significant reduction ($P<0.001$) in the number of leaking spots (corresponding to newly formed immature microvessels with leakage of fluorescein) in MMP-2,9 double KO mice compared with MMP-2 or MMP-9 deficient mice. This corresponded to a strong inhibition of neovascular progression estimated at day 14 after induction by immunostaining with anti-PECAM antibodies in MMP-2,9 double KO mice ([Fig. 1D](#)), compared with MMP-2 or MMP-9 deficient ([Fig. 1B-C](#)) or WT ([Fig. 1A](#)) animals. We then quantified choroidal pathological reaction in sites developing a neovascular membrane by measuring, on serial sections, the maximal height of the lesion above the choroidal layer observed in neighboring intact zones. This was performed by determining the B/C ratio between total thicknesses of lesions (B, from the bottom of the choroid to the top of the neovascular area) to the thickness of adjacent normal choroid (C) according to Lambert et al. (24, 25). A significant reduction of the B/C ratio was observed in MMP-9 (33%), MMP-2 (44%), and MMP-2,9 (56%) deficient mice compared with their corresponding WT ($P<0.001$, [Fig. 1E](#)).

Presence of MMP-2 and MMP-9 in the posterior segments of WT and MMP deficient mice at day 5 and temporal profile during the formation of choroidal neovascularization

Ocular posterior segment proteins prepared from WT, MMP-9 KO, MMP-2 KO, and MMP-2,9 KO mice were analyzed by gelatin zymography ([Fig. 2A](#)). As expected, no MMP-2 and MMP-9 activity was detected in MMP-2 KO, MMP-9 KO, and MMP-2,9 KO mice (not shown), respectively. WT mice expressed pro-MMP-2 and -MMP-9 as well as processed MMP-2. Although the ocular expression of MMP-9 increased in the MMP-2 KO mice, MMP-2 KO mice were significantly protected from the development of severe choroidal neovascularization. Both pro-MMP-2 and pro-MMP-9 progressively accumulated during the early stages of choroidal neovascularization formation, with the appearance of active forms of MMP-2 ([Fig. 2B](#)).

In situ zymography revealed that gelatinase activation in the posterior ocular segments was predominantly present in the area developing choroidal neovascularization ([Fig. 2C](#)). Although gelatinolytic activity was strongly decreased in double MMP-2,9 deficient mice, residual activity was still detectable at the top of the choroidal pathological reaction ([Fig. 2D](#)).

Kinetics of MMP expression

To evaluate the level of regulation, we first analyzed the temporal profiles of MMP-2 and MMP-9 expression by semiquantitative RT-PCR. MMP-9 expression was upregulated during early phases of choroidal neovascularization formation, whereas MMP-2 (constitutively expressed) showed no significant modulation ([Fig. 3A-B](#)). We knew from previous work (36) that members of the plasminogen system are induced early during the process (important for plasmin-mediated activation of pro-MMP-9). The presence of active forms of MMP-2 theoretically could correspond either to a decrease of TIMP expression or to an increase in the expression of activators (MT1-MMP). RT-PCR analysis demonstrated a constant expression of TIMP-2 but a significant upregulation of MT1-MMP mRNA ([Fig. 3, B and C](#)).

Effect of MMP deficiency on fibrinolytic activity

Plasminogen activators/plasmin play an important role in choroidal neovascularization (24, 36). However, MMPs may modulate fibrinolysis through plasminogen-dependent or independent mechanisms (37–39). We evaluated the immunohistochemical staining of fibrinogen/fibrin, as an endpoint of fibrinolytic activity. This demonstrated the presence of similar fibrinogen/fibrin deposits in WT and MMP-2 or MMP-9 deficient mice ([Fig. 4A-C](#)). However, fibrinogen/fibrin accumulated in double MMP-2,9 deficient animals, suggesting that the absence of both gelatinases impaired fibrinolytic activity in the choroidal neovascular membrane ([Fig. 4D](#)).

MMP inhibitors decrease the development of choroidal neovascularization

In a second approach to show that MMPs contribute to the development of choroidal neovascularization, we induced endogenous overexpression of TIMP-1 or TIMP-2 with adenoviral-mediated delivery in WT mice. RT-PCR analysis of murine posterior segments revealed that systemic intravenous injections also led to increased local expressions of TIMP-1 and TIMP-2 ([Fig. 5A-B](#)). Evaluation by in situ zymography demonstrated a complete inhibition of gelatinolytic activity after AdTIMP-1 injections, whereas residual activity was still present in case of AdTIMP-2 ([Fig. 5C-D](#)). The evaluation of choroidal neovascularization formation by B/C ratio calculation was compared on serial frozen sections in WT mice 14 days after injection with either AdTIMP-1 or AdTIMP-2. Both TIMP-1 and TIMP-2 overexpression significantly reduced angiogenesis ($P < 0.001$) compared with WT controls injected with AdRR5 ([Fig. 5E](#)).

We then evaluated the consequences of broad spectrum (BB-94) or more selective MMP inhibitor (Ro 28-2653, a more selective synthetic gelatinase inhibitor acting preferentially on MMP-2, MMP-9, and MT1-MMP, ref. 35) inhibition on choroidal neovascularization development by treating WT mice with daily systemic injections. Both inhibitors significantly reduced the choroidal neovascularization formation. ([Fig. 5F](#)). However, Ro 28-2653 was more efficient ($P < 0.001$) than BB-94. Interestingly, selective MMP inhibition treatment started 5 days after laser induction also significantly inhibited the development of choroidal angiogenesis (40% inhibition) indicating thereby a potential for drug-induced regression ([Fig. 5F](#)).

DISCUSSION

This study shows that both MMP-2 and MMP-9 cooperate in the course of experimental choroidal neovascularization. Indeed, choroidal pathological angiogenesis was nearly fully

prevented in MMP-2/MMP-9 double deficient mice, whereas it was only partly impaired in the single MMP deficient mice ([Fig. 1D-F](#)). These results were supported by the strong inhibition of choroidal angiogenesis in mice treated with a selective gelatinase/MT1-MMP synthetic inhibitor ([Fig. 5F](#)).

Previous studies suggested a role for different MMPs in the exudative form of AMD (22–24, 26, 40–41). With the use of MMP deficient mice (MMP-2 KO, MMP-9 KO, and MMP-2,9 KO) and different methods of MMP inhibition (AdTIMP-1, AdTIMP-2, BB-94, and Ro 28-2653), our observations provide a more complete understanding of the role of the MMP system in choroidal neovascularization. MMP-9 mRNA was upregulated, whereas MMP-2 mRNA showed little variation during choroidal neovascularization formation. However, MT1-MMP, which is a major MMP-2 activator, was strongly induced (10, 11, 42). It is of interest to note that in our model, MMP-2 deficiency was accompanied by increased MMP-9 activity detected by gelatin zymography, while the opposite was not observed. However, this increase in MMP-9 did not prevent the inhibitory consequences of MMP-2 deficiency on choroidal neovascularization development ([Fig. 1](#)).

Fibrin and other adhesive proteins such as vitronectin, laminin, and fibronectin form a provisional matrix, which supports angiogenesis (43). We have recently demonstrated the importance of finely tuned fibrinolysis for the development of subretinal pathological angiogenesis (25, 36). However, both excessive (in PAI-1 deficient mice) and deficient fibrinolysis (in plasminogen deficient mice) prevent the formation of laser-induced choroidal neovascular membranes. The plasminogen/plasminogen activator system is not the only way of regulating fibrinolysis. Indeed, a similar role has been demonstrated for members of the MMP system. In antglomerular basement membrane nephritis, MMP-9 is required for fibrinolysis, and in its absence, fibrin accumulates in glomeruli (44). We observed that the combined absence of both gelatinases resulted in an accumulation of fibrin in laser-induced lesions, which could present a physical barrier to the infiltrating cellular components of choroidal neovascularization (endothelial cells, fibroblasts, and mononuclear cells). We did not detect mononuclear cells in MMP-2,9 deficient mice by immunostaining with MAC-3 antibody, while these inflammatory cells were always present at the migrating border of the neovascular membrane in WT controls (not shown).

Is there a place for MMP inhibition in the treatment of choroidal neovascularization? Although TIMP-3 has efficacy for the inhibition of the pathological process (45), it also has proapoptotic properties, which obviously limit its therapeutic potential in a senescent eye (46). Accordingly, we therefore evaluated the effects of TIMP-1 and TIMP-2 with adenoviral delivery. Although TIMP-2 overexpression was less efficient than TIMP-1 for the inhibition of in situ gelatinolytic activity, it was more effective in preventing the formation of the choroidal reaction. Whether this affects the ability of TIMP-2, but not TIMP-1, to inhibit MT1-MMP (42), which is also induced in early stages of choroidal neovascularization, formation remains to be determined. MT1-MMP could act either through its fibrinolytic activity or through its capacity to activate MMP-2 to facilitate choroidal neovascularization. Unfortunately, our experimental model cannot be applied to MT1-MMP deficient mice, which die shortly after birth (47). A synthetic MMP inhibitor interacting preferentially with MMP-2, MMP-9, and MT1-MMP (Ro 28-2653) inhibited the choroidal neovascularization more effectively than the nonspecific inhibitor ([Fig. 5F](#)). It is of interest to note that similar observations have recently been reported in a tumor model (48). This

suggests that broad spectrum inhibition of MMP activity might also repress some beneficial MMP effects (49). Indeed, RT-PCR analysis (unpublished data) showed that other MMPs (including MMP-8, MMP-12, and MMP-19) are expressed during choroidal neovascularization formation the role of which in the disease is at present unknown. MMPs can stimulate angiogenesis or generate antiangiogenic factors (such as angiostatin or endostatin) and degrade basement membranes, which may limit the extent of angiogenesis at a later stage by destabilizing the newly formed blood vessels (10, 11, 50). Altogether, these results suggest that a selective inhibition of only some MMPs might be more efficient than an inhibition of the complete MMP repertoire for angiogenesis control.

In conclusion, we have shown that MMP-2 and MMP-9 cooperate in experimental laser-induced choroidal neovascularization. In mice with a combined deficiency of both MMP-2 and MMP-9 genes, both the incidence and the severity of the pathological choroidal reaction were significantly reduced, highlighting the differences between physiological (double knockouts developed normally) and pathological angiogenesis (51). Since a selective MMP synthetic inhibitor could also effectively inhibit subretinal angiogenesis, we believe that inhibition of MMP-2, MMP-9, and MT1-MMP may represent a promising strategy for the treatment or for the prevention of the exudative form of age-related macular degeneration.

ACKNOWLEDGMENTS

We thank L. Naa and F. Olivier for collaboration and P. Gavitelli for technical assistance. B. Wielockx and C. Libert kindly provided the double genes MMP-2,9 deficient mice and fluorescein-conjugated gelatin, Z. Werb the MMP-9, and T. Itoh the MMP-2 knockouts. C. Galopin and M. Jost contributed to establish the zymography technique in our laboratory. These studies were supported by funds from Les Amis des Aveugles (Ghlin), the Fonds de la Recherche Scientifique Médicale (FRSM), the Fonds National de la Recherche Scientifique (FNRS, Belgium), and The Steinbach Foundation (to Z. Werb). C. Munaut is a research associate and A. Noël is a senior research associate from the National Fund for Scientific Research (FNRS), Belgium.

REFERENCES

1. Fine, S. L., Berger, J. W., Maguire, M. G., and Ho, A. C. (2000) Age-related macular degeneration. *N. Engl. J. Med.* **342**, 483–492
2. VanNewkirk, M. R., Nanjan, M. B., Wang, J. J., Mitchell, P., Taylor, H. R., and McCarty, C. A. (2000) The prevalence of age-related maculopathy: the visual impairment project. *Ophthalmology* **107**, 1593–1600
3. Campochiaro, P. A. (2000) Retinal and choroidal neovascularization. *J. Cell. Physiol.* **184**, 301–310
4. Carmeliet, P., and Jain, R. K. (2000) Angiogenesis in cancer and other diseases. *Nature* **407**, 249–257
5. Schwesinger, C., Yee, C., Rohan, R. M., Joussen, A. M., Fernandez, A., Meyer, T. N., Poulaki, V., Ma, J. J., Redmond, T. M., Liu, S., et al. (2001) Intrachoroidal

neovascularization in transgenic mice overexpressing vascular endothelial growth factor in the retinal pigment epithelium. *Am. J. Pathol.* **158**, 1161–1172

6. Ogata, N., Wada, M., Otsuji, T., Jo, N., Tombran-Tink, J., and Matsumura, M. (2002) Expression of pigment epithelium-derived factor in normal adult rat eye and experimental choroidal neovascularization. *Invest. Ophthalmol. Vis. Sci.* **43**, 1168–1175
7. Dawson, D. W., Volpert, O. V., Gillis, P., Crawford, S. E., Xu, H., Benedict, W., and Bouck, N. P. (1999) Pigment epithelium-derived factor: a potent inhibitor of angiogenesis. *Science* **285**, 245–248
8. Krzystolik, M. G., Afshari, M. A., Adamis, A. P., Gaudreault, J., Gragoudas, E. S., Michaud, N. A., Li, W., Connolly, E., O'Neill, C. A., and Miller, J. W. (2002) Prevention of experimental choroidal neovascularization with intravitreal anti-vascular endothelial growth factor antibody fragment. *Arch. Ophthalmol.* **120**, 338–346
9. Mori, K., Gehlbach, P., Ando, A., McVey, D., Wei, L., and Campochiaro, P. A. (2002) Regression of ocular neovascularization in response to increased expression of pigment epithelium-derived factor. *Invest. Ophthalmol. Vis. Sci.* **43**, 2428–2434
10. Egeblad, M., and Werb, Z. (2002) New functions for the matrix metalloproteinases in cancer progression. *Nat. Rev. Cancer* **2**, 161–174
11. Overall, C. M., and Lopez-Otin, C. (2002) Strategies for MMP inhibition in cancer: innovations for the post-trial era. *Nat. Rev. Cancer* **2**, 657–672
12. Holmbeck, K., Bianco, P., Caterina, J., Yamada, S., Kromer, M., Kuznetsov, S. A., Mankani, M., Robey, P. G., Poole, A. R., Pidoux, I., et al. (1999) MT1-MMP-deficient mice develop dwarfism, osteopenia, arthritis, and connective tissue disease due to inadequate collagen turnover. *Cell* **99**, 81–92
13. Vu, T. H., Shipley, J. M., Bergers, G., Berger, J. E., Helms, J. A., Hanahan, D., Shapiro, S. D., Senior, R. M., and Werb, Z. (1998) MMP-9/gelatinase B is a key regulator of growth plate angiogenesis and apoptosis of hypertrophic chondrocytes. *Cell* **93**, 411–422
14. Shapiro, S. D. (1998) Matrix metalloproteinase degradation of extracellular matrix: biological consequences. *Curr. Opin. Cell Biol.* **10**, 602–608
15. Lund, L. R., Romer, J., Bugge, T. H., Nielsen, B. S., Frandsen, T. L., Degen, J. L., Stephens, R. W., and Dano, K. (1999) Functional overlap between two classes of matrix-degrading proteases in wound healing. *EMBO J.* **18**, 4645–4656
16. Carmeliet, P., Moons, L., Lijnen, R., Baes, M., Lemaître, V., Tipping, P., Drew, A., Eeckhout, Y., Shapiro, S., Lupu, F., et al. (1997) Urokinase-generated plasmin activates matrix metalloproteinases during aneurysm formation. *Nat. Genet.* **17**, 439–444
17. Chang, C., and Werb, D. (2001) The many faces of metalloproteases: cell growth, invasion, angiogenesis and metastasis. *Trends Cell Biol.* **11**, S37–S43

18. Manes, S., Llorente, M., Lacalle, R. A., Gomez-Mouton, C., Kremer, L., Mira, E., and Martinez, A. C. (1999) The matrix metalloproteinase-9 regulates the insulin-like growth factor-triggered autocrine response in DU-145 carcinoma cells. *J. Biol. Chem.* **274**, 6935–6945
19. Bergers, G., Brekken, R., McMahon, G., Vu, T. H., Itoh, T., Tamaki, K., Tanzawa, K., Thorpe, P., Itohara, S., Werb, Z., et al. (2000) Matrix metalloproteinase-9 triggers the angiogenic switch during carcinogenesis. *Nat. Cell Biol.* **2**, 737–744
20. Dong, Z., Kumar, R., Yang, X., and Fidler, I. J. (1997) Macrophage-derived metalloelastase is responsible for the generation of angiostatin in Lewis lung carcinoma. *Cell* **88**, 801–810
21. Das, A., McGuire, P. G., Eriqat, C., Ober, R. R., DeJuan, E., Jr., Williams, G. A., McLamore, A., Biswas, J., and Johnson, D. W. (1999) Human diabetic neovascular membranes contain high levels of urokinase and metalloproteinase enzymes. *Invest. Ophthalmol. Vis. Sci.* **40**, 809–813
22. Kadonosono, K., Yazama, F., Itoh, N., Sawada, H., and Ohno, S. (1999) Expression of matrix metalloproteinase-7 in choroidal neovascular membranes in age-related macular degeneration. *Am. J. Ophthalmol.* **128**, 382–384
23. Weber, B., Vogt, G., Pruetz, R. C., Stohr, H., and Felbor, U. (1994) Mutations in the tissue inhibitor of metalloproteinases-3 (TIMP3) in patients with Sorsby's fundus dystrophy. *Nat. Genet.* **8**, 352–356
24. Lambert, V., Munaut, C., Jost, M., Noel, A., Werb, Z., Foidart, J. M., and Rakic, J. M. (2002) Matrix metalloproteinase-9 contributes to choroidal neovascularization. *Am. J. Pathol.* **161**, 1247–1253
25. Lambert, V., Munaut, C., Noel, A., Frankenne, F., Bajou, K., Gerard, R., Carmeliet, P., Defresne, M. P., Foidart, J. M., and Rakic, J. M. (2001) Influence of plasminogen activator inhibitor type 1 on choroidal neovascularization. *FASEB J.* **15**, 1021–1027
26. Steen, B., Sejersen, S., Berglin, L., Seregard, S., and Kvanta, A. (1998) Matrix metalloproteinases and metalloproteinase inhibitors in choroidal neovascular membranes. *Invest. Ophthalmol. Vis. Sci.* **39**, 2194–2200
27. Kvanta, A., Shen, W. Y., Sarman, S., Seregard, S., Steen, B., and Rakoczy, E. (2000) Matrix metalloproteinase (MMP) expression in experimental choroidal neovascularization. *Curr. Eye Res.* **21**, 684–690
28. Longo, G. M., Xiong, W., Greiner, T. C., Zhao, Y., Fiotti, N., and Baxter, B. T. (2002) Matrix metalloproteinases 2 and 9 work in concert to produce aortic aneurysms. *J. Clin. Invest.* **110**, 625–632
29. Itoh, T., Matsuda, H., Tanioka, M., Kuwabara, K., Itohara, S., and Suzuki, R. (2002) The role of matrix metalloproteinase-2 and matrix metalloproteinase-9 in antibody-induced arthritis. *J. Immunol.* **169**, 2643–2647

30. Itoh, T., Ikeda, T., Gomi, H., Nakao, S., Suzuki, T., and Itohara, S. (1997) Unaltered secretion of β -amyloid precursor protein in gelatinase A (matrix metalloproteinase 2)-deficient mice. *J. Biol. Chem.* **272**, 22389-22392
31. Munaut, C., Noel, A., Weidle, U. H., Krell, H. W., and Foidart, J. M. (1995) Modulation of the expression of interstitial and type-IV collagenases in coculture of HT1080 fibrosarcoma cells and fibroblasts. *Invasion Metastasis* **15**, 169-178
32. Pagenstecher, A., Stalder, A. K., Kincaid, C. L., Volk, B., and Campbell, I. L. (2000) Regulation of matrix metalloproteinases and their inhibitor genes in lipopolysaccharide-induced endotoxemia in mice. *Am. J. Pathol.* **157**, 197-210
33. Baker, A. H., Zaltsman, A. B., George, S. J., and Newby, A. C. (1998) Divergent effects of tissue inhibitor of metalloproteinase-1, -2, or -3 overexpression on rat vascular smooth muscle cell invasion, proliferation, and death in vitro. TIMP-3 promotes apoptosis. *J. Clin. Invest.* **101**, 1478-1487
34. Carmeliet, P., Moons, L., Lijnen, R., Janssens, S., Lupu, F., Collen, D., and Gerard, R. D. (1997) Inhibitory role of plasminogen activator inhibitor-1 in arterial wound healing and neointima formation: a gene targeting and gene transfer study in mice. *Circulation* **96**, 3180-3191
35. Lein, M., Jung, K., Ortel, B., Stephan, C., Rothaug, W., Juchem, R., Johannsen, M., Deger, S., Schnorr, D., Loening, S., et al. (2002) The new synthetic matrix metalloproteinase inhibitor (Roche 28-2653) reduces tumor growth and prolongs survival in a prostate cancer standard rat model. *Oncogene* **21**, 2089-2096
36. Rakic, J. M., Lambert, V., Munaut, C., Bajou, K., Peyrollier, K., Alvarez-Gonzalez, M. L., Carmeliet, P., Foidart, J. M., and Noël, A. (2003) Mice lacking uPA, tPA or Plasminogen genes are resistant to experimental choroidal neovascularization. *Invest. Ophthalmol. Vis. Sci.* **44**, 1732-1739
37. Lijnen, H. R. (2002) Matrix metalloproteinases and cellular fibrinolytic activity. *Biochemistry (Mosc.)* **67**, 92-98
38. Pepper, M. S. (2001) Role of the matrix metalloproteinase and plasminogen activator-plasmin systems in angiogenesis. *Arterioscler. Thromb. Vasc. Biol.* **21**, 1104-1117
39. Hiraoka, N., Allen, E., Apel, I. J., Gyetko, M. R., and Weiss, S. J. (1998) Matrix metalloproteinases regulate neovascularization by acting as pericellular fibrinolysins. *Cell* **95**, 365-377
40. Qi, J. H., Ebrahim, Q., Yeow, K., Edwards, D. R., Fox, P. L., and Anand-Apte, B. (2002) Expression of Sorsby's fundus dystrophy mutations in human retinal pigment epithelial cells reduces matrix metalloproteinase inhibition and may promote angiogenesis. *J. Biol. Chem.* **277**, 13394-13400

41. Berglin, L., Sarman, S., van der Ploeg, I., Steen, B., Ming, Y., Itohara, S., Seregard, S., and Kvanta, A. (2003) Reduced choroidal neovascular membrane formation in matrix metalloproteinase-2-deficient mice. *Invest. Ophthalmol. Vis. Sci.* **44**, 403–408
42. Brew, K., Dinakarbandian, D., and Nagase, H. (2000) Tissue inhibitors of metalloproteinases: evolution, structure and function. *Biochim. Biophys. Acta* **1477**, 267–283
43. Dvorak, H. F., Brown, L. F., Detmar, M., and Dvorak, A. M. (1995) Vascular permeability factor/vascular endothelial growth factor, microvascular hyperpermeability, and angiogenesis. *Am. J. Pathol.* **146**, 1029–1039
44. Lelongt, B., Bengatta, S., Delauche, M., Lund, L. R., Werb, Z., and Ronco, P. M. (2001) Matrix metalloproteinase 9 protects mice from anti-glomerular basement membrane nephritis through its fibrinolytic activity. *J. Exp. Med.* **193**, 793–802
45. Takahashi, T., Nakamura, T., Hayashi, A., Kamei, M., Nakabayashi, M., Okada, A. A., Tomita, N., Kaneda, Y., and Tano, Y. (2000) Inhibition of experimental choroidal neovascularization by overexpression of tissue inhibitor of metalloproteinases-3 in retinal pigment epithelium cells. *Am. J. Ophthalmol.* **130**, 774–781
46. Majid, M. A., Smith, V. A., Easty, D. L., Baker, A. H., and Newby, A. C. (2002) Sorsby's fundus dystrophy mutant tissue inhibitors of metalloproteinase-3 induce apoptosis of retinal pigment epithelial and MCF-7 cells. *FEBS Lett.* **529**, 281–285
47. Holmbeck, K., Bianco, P., Caterina, J., Yamada, S., Kromer, M., Kuznetsov, S. A., Mankani, M., Robey, P. G., Poole, A. R., Pidoux, I., et al. (1999) MT1-MMP-deficient mice develop dwarfism, osteopenia, arthritis, and connective tissue disease due to inadequate collagen turnover. *Cell* **99**, 81–92
48. Arlt, M., Kopitz, C., Pennington, C., Watson, K. L., Krell, H. W., Bode, W., Gansbacher, B., Khokha, R., Edwards, D. R., and Kruger, A. (2002) Increase in gelatinase-specificity of matrix metalloproteinase inhibitors correlates with antimetastatic efficacy in a T-cell lymphoma model. *Cancer Res.* **62**, 5543–5550
49. Jiang, Y., Goldberg, I. D., and Shi, Y. E. (2002) Complex roles of tissue inhibitors of metalloproteinases in cancer. *Oncogene* **21**, 2245–2252
50. Yamada, E., Tobe, T., Yamada, H., Okamoto, N., Zack, D. J., Werb, Z., Soloway, P. D., and Campochiaro, P. A. (2001) TIMP-1 promotes VEGF-induced neovascularization in the retina. *Histol. Histopathol.* **16**, 87–97
51. Carmeliet, P. (2000) Mechanisms of angiogenesis and arteriogenesis. *Nat. Med.* **6**, 389–395

Received May 9, 2003; accepted August 11, 2003.

Table 1**RT-PCR parameters**

Gene and accession number	Position	Oligonucleotide sequence (5'-3')	Size of PCR Product	Number of cycles
28S U13369	12403F 12614R	G TTCACCCACTAATAGGGAACGTGA G GATTCTGACTTAGAGGCCGTTCACT	212 bp	19
h, m MMP-2 NM_004530 NM_008610	1740F (h) or 1500F (m) 1964R (h) or 1724R (m)	A GATCTTCTTCTTCAAGGACCGGTT G GCTGGTCAGTGGCTTGGGGTA	225 bp	35
h MMP-9 NM_004994	1592F 1800R	G C G G A G A T T G G G A A C C A G C T G T A G A C G C G C C T G T G T A C A C C C A C A	209 bp	35
m MMP-9 NM_013599	1612F 1819R	G T T T T T G A T G C T A T T G C T G A G A T C C A C C C A C A T T T G A C G T C C A G A G A A G A A	208 bp	35
h TIMP-1 X03124	93F 259R	C A T C C T G T T G T T G C T G T G G C T G A T G T C A T C T T G A T C T C A T A A C G C T G G	167 bp	35
m TIMP-1 X04684	137F 306R	G G C A T C C T C T T G T T G C T A T C A C T G G T C A T C T T G A T C T C A T A A C G C T G G	169 bp	35
h, m TIMP-2 J05593 (h) M93954 (m)	570F (h) or 308F (m) 724R (h) or 462R (m)	C T C G C T G G A C G T T G G A G G A A A G A A A G C C C A T C T G G T A C C T G T G G T T C A	155 bp	35
h,m MT1-MMP NM_004995 X83536	1288F (h) or 1226F (m) 1508R (h) or 1446R (m)	G G A T A C C C A A T G C C C A T T G G C C A C C A T T G G G C A T C C A G A A G A G A G C	221 bp	35

Fig. 1

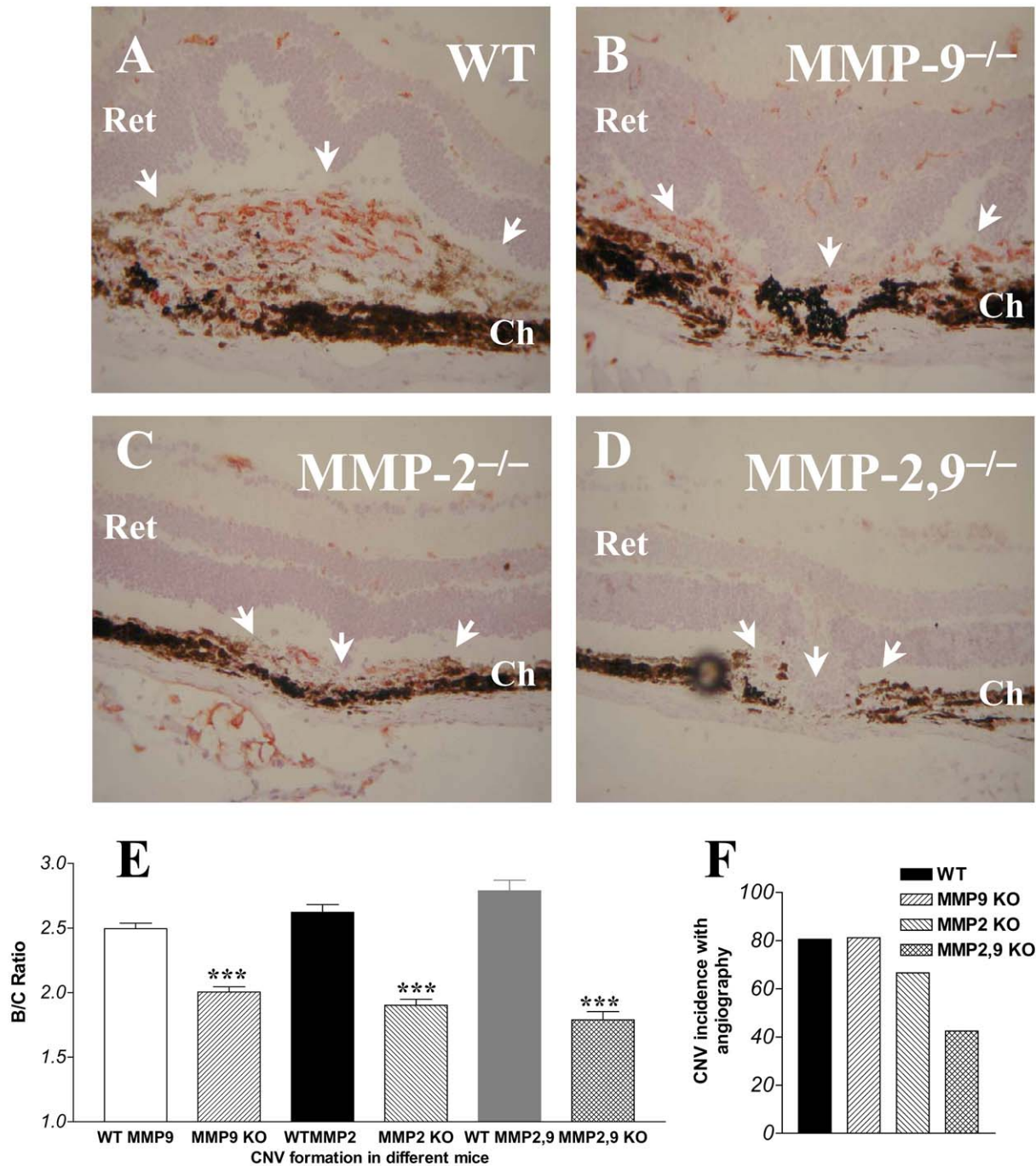


Figure 1. Absence of MMP-2 and MMP-9 prevents the development of experimental choroidal neovascularization.

Hematoxylin-eosin staining of a representative area of choroidal neovascularization at the site of laser-induced trauma in control (A) or in mice deficient for MMP-9 (B), MMP-2 (C), and both MMP-2,9 (D). Almost complete absence of neovascularization is visible in mice deficient for both MMP-2 and MMP-9 when vessels were immunostained with anti-mouse PECAM antibody (immunostained in orange with AEC) compared with other conditions, confirming thereby the reduced incidence of neovascularization calculated before death by fluorescein angiography evaluation of the number of leaking laser spots (F). Neovascular reaction was determined with computer-assisted image analysis by evaluating the B/C ratio as described previously (24, 25) at day 14 after laser injury of the Bruch's membrane in single/double deficient mice and in the corresponding WT controls (E). The neural retina (ret) and choroidal layer (ch) are indicated, and the neovascular area is arrowed. *** $P < 0.001$; error bars = SE. Original magnification = x200.

Fig. 2

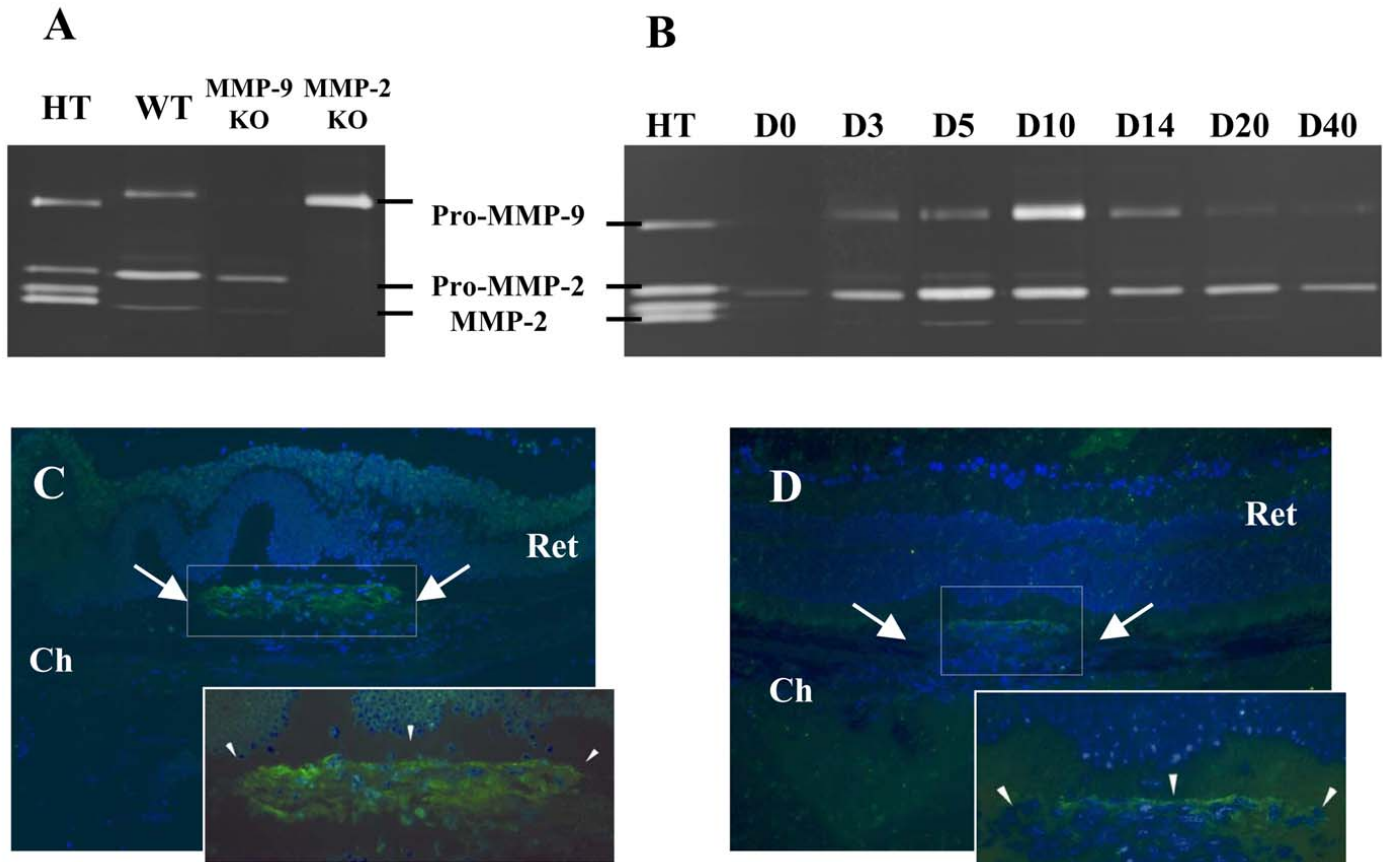


Figure 2. Zymographic analysis of MMP-2 and MMP-9 in knockouts and WT mice. At day 5 after the induction of choroidal neovascularization by laser, animals were killed and posterior segment extract samples (5 ng/lane) from eyes of WT and MMP-2 or MMP-9 deficient mice were analyzed by gelatin zymography (**A**). As positive control, medium conditioned by human HT1080 cells was included ("HT"). Data are the results of a single experiment, which was 1 of 3 with similar results. In WT mice, a kinetic zymographic evaluation was also performed at different intervals after laser-induced CNV demonstrating a temporal increase in pro-MMP-9 and the appearance of active forms of MMP-2 (**B**). In situ zymography with fluorescein-conjugated gelatin demonstrates the concentration of gelatinolytic activity at the level of the neovascular membrane growing under the retina (**C**), with limited residual activity at the top of the membrane in double MMP-2,9 deficient mice (**D**). The neural retina (ret) and choroidal layer (Ch) are indicated, and arrows indicate the neovascular area. Original magnification = x200 and x400.

Fig. 3

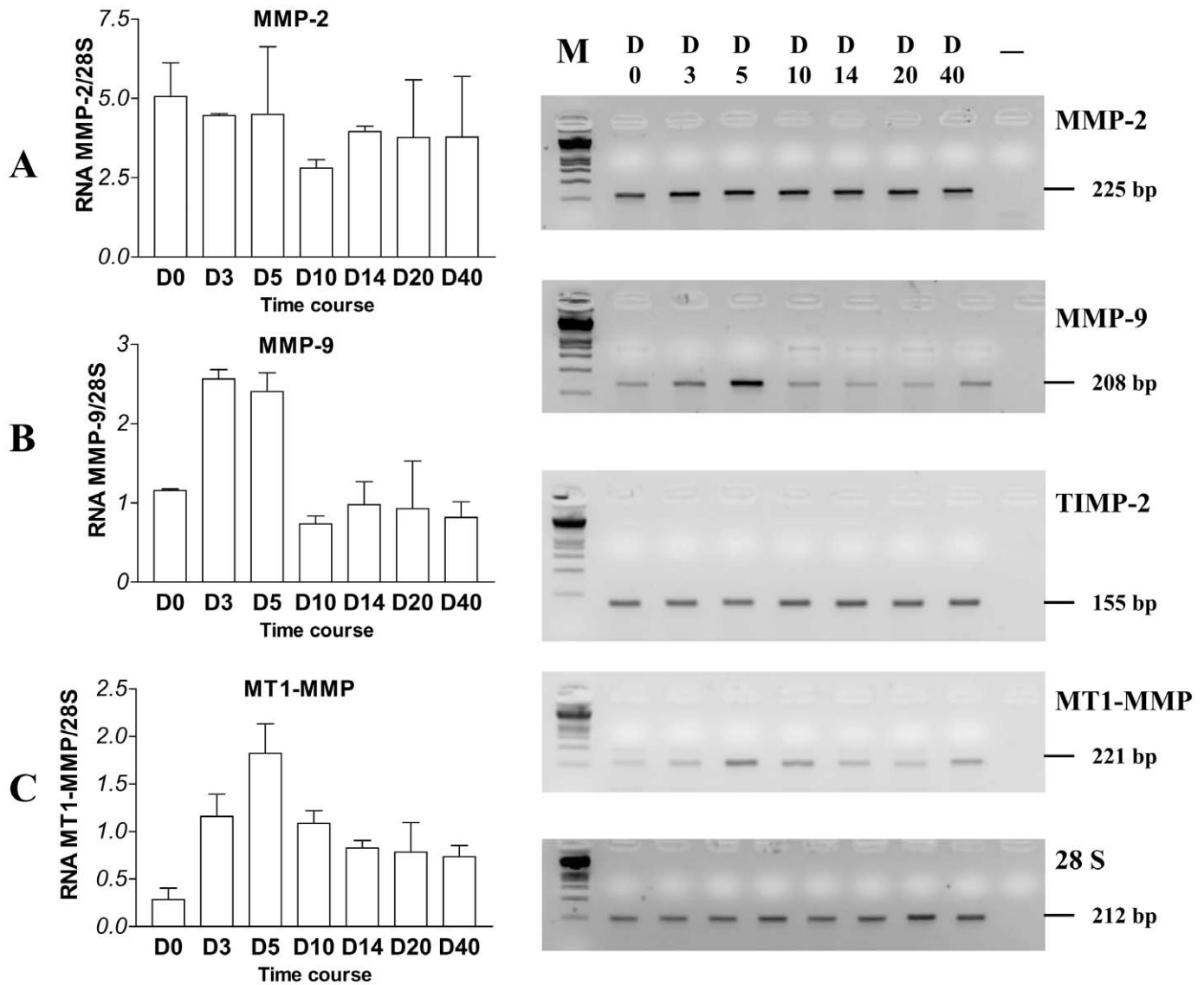


Figure 3. Kinetic evaluation of MMP expression by semiquantitative RT-PCR during the development of experimental CNV. The histograms correspond to the densitometric quantification of MMP-2 (A), MMP-9 (B), and MT1-MMP (C) mRNA normalized to the 28S signal at different endpoints. Evaluation was performed on the entire posterior segment after the induction of multiple wounds to Bruch's membrane. Unlike MMP-2 and TIMP-2 (histogram not shown), which remained relatively constant, MMP-9 and MT1-MMP mRNA expression appeared to be induced during the early phases of CNV development. Representative gels are displayed with RT-PCR products expected size (bp) at right.

Fig. 4

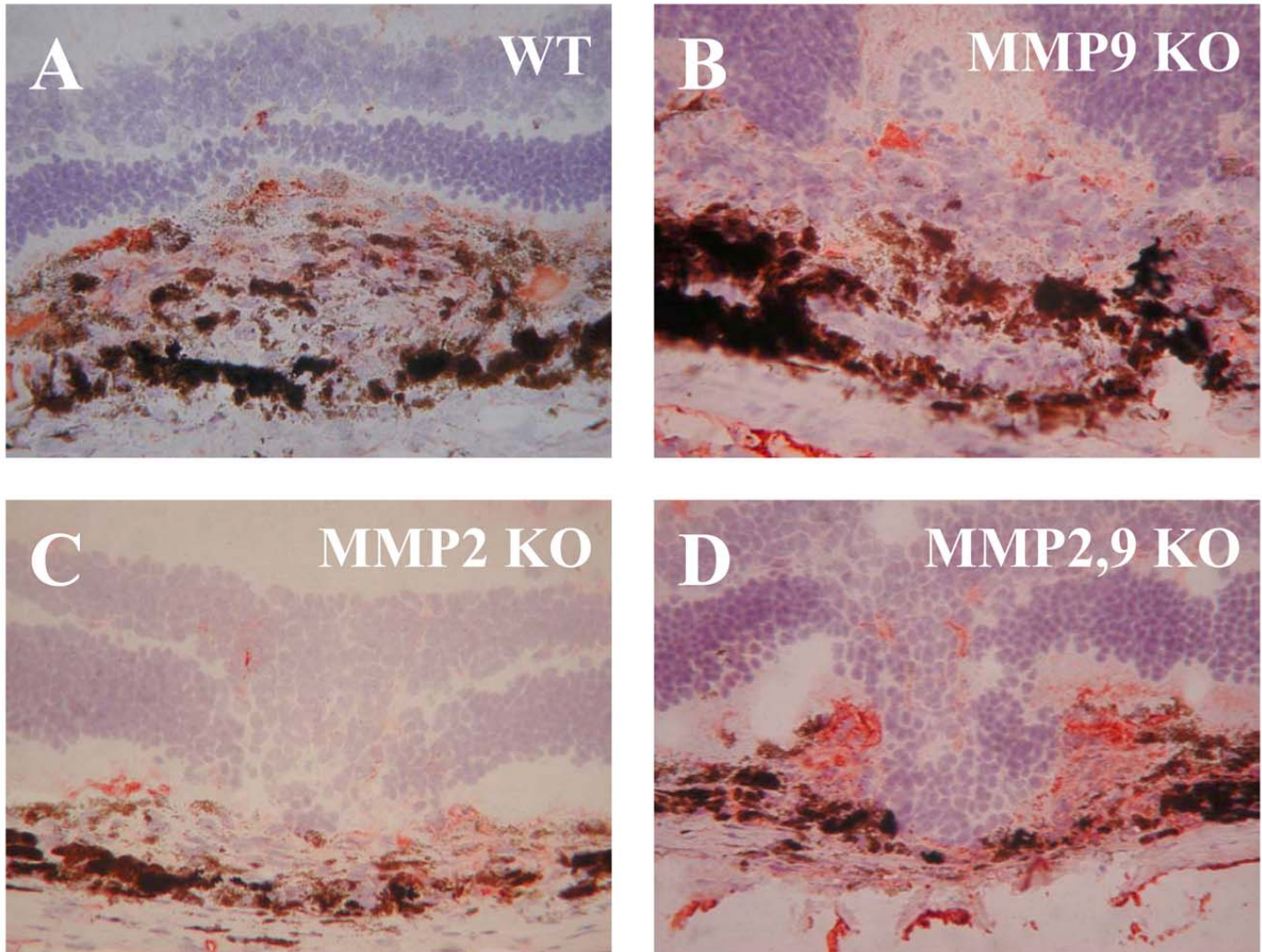


Figure 4. Immunohistochemical staining for fibrinogen/fibrin at the site of laser-induced wound in WT and deficient mice. Frozen ocular sections from wild-type (*A*), MMP-9^{-/-} (*B*), and MMP-2^{-/-} (*C*) mice reveal the presence of limited amount of fibrin (stained in orange with AEC) in WT mice or single MMP gene-deficient mice contrasting with the accumulation of fibrin at the site of restricted choroidal reaction observed in double gene MMP-2,9 deficient animals (*D*). Original magnification = x400.

Fig. 5

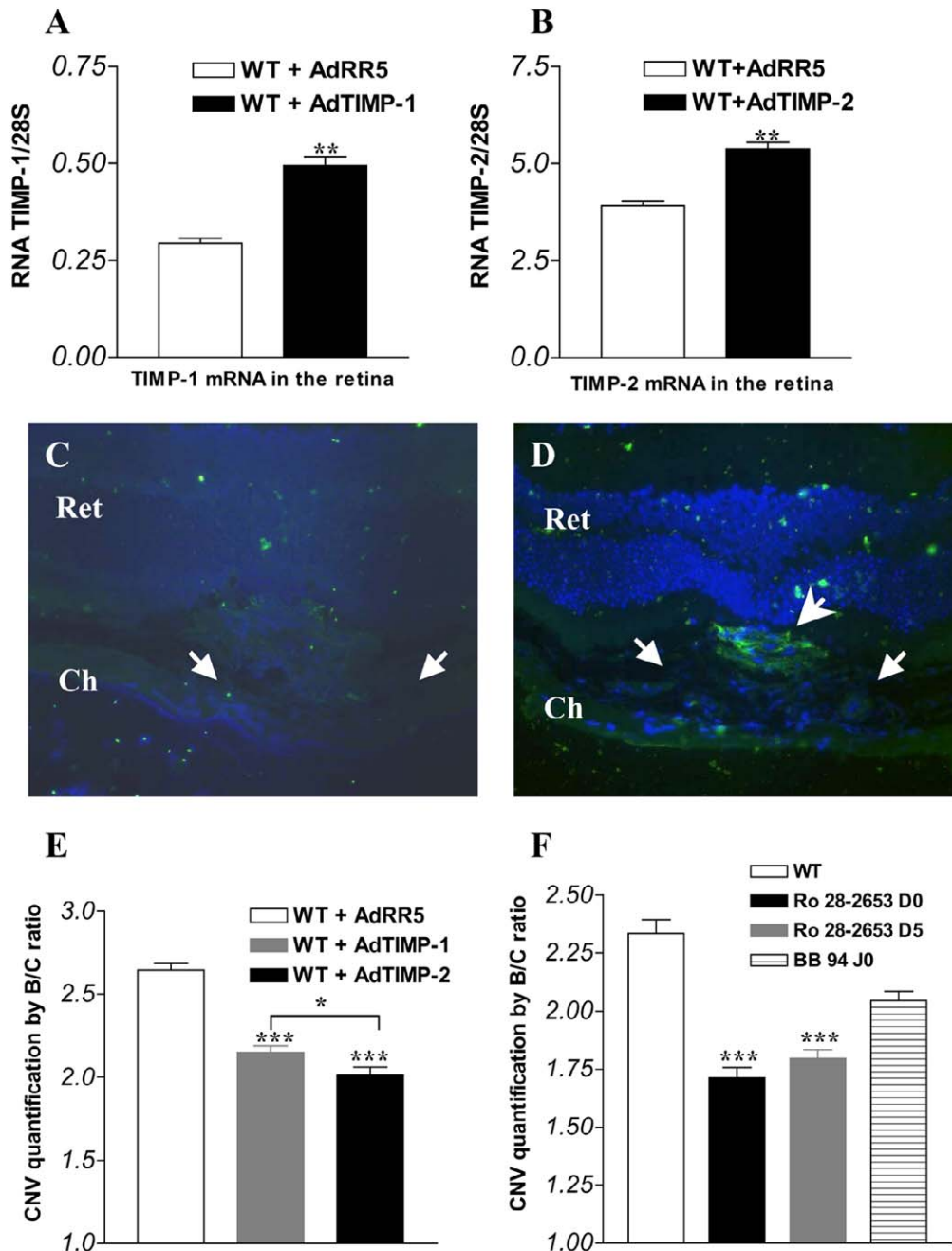


Figure 5. Decreased CNV formation with endogenous or synthetic MMP inhibitors. Systemic injection of adenoviral vectors carrying recombinant human TIMP-1 or TIMP-2 resulted in local overexpression of these MMP inhibitors demonstrated by semiquantitative RT-PCR analysis of injected mice compared with animals injected with control AdRR5 virus (**A-B**). Analysis was performed on posterior ocular segments at day 5 after laser-induced choroidal neovascularization. In situ zymographic evaluation demonstrates a complete inhibition of gelatinolytic activity with AdTIMP-1 transduction, contrasting with signs of residual gelatinolysis with AdTIMP-2 (**C-D**). Evaluation of the choroidal neovascular reaction by B/C ratio calculation showed that both TIMP-1 and TIMP-2 overexpression significantly reduced the pathological reaction. TIMP-2 adenoviral-mediated delivery seemed to be more efficient ($P < 0.05$) than TIMP-1 local overexpression (**E**). Evaluation of pharmacological inhibition of MMPs on choroidal pathological angiogenesis demonstrated that a selective gelatinase and MT1-MMP synthetic inhibitor administered with daily intraperitoneal injections at day 0 or at day 5 after laser induction was much more efficient ($P < 0.001$) than a broad spectrum inhibitor (BB-94) (**F**). The neural retina (ret), and choroidal layer (Ch) are indicated, and the neovascular area is arrowed. *** $P < 0.001$; ** $P < 0.01$; * $P < 0.05$; error bars = SE. Original magnification = x200.